The Journal of Experimental Biology 212, 3564-3575
Published by The Company of Biologists 2009
doi:10.1242/jeb.029512

Allometry of skeletal muscle fine structure allows maintenance of aerobic capacity during ontogenetic growth

Steven Young and Stuart Egginton*

Department of Physiology, University of Birmingham, Vincent Drive, Edgbaston, Birmingham B15 2TT, UK

*Author for correspondence (s.egginton@bham.ac.uk)

Accepted 6 August 2009

SUMMARY

Controversy exists over the scaling of oxygen consumption with body mass in vertebrates. A combination of biochemical and structural analyses were used to examine whether individual elements influencing oxygen delivery and demand within locomotory muscle respond similarly during ontogenetic growth of striped bass. Mass-specific metabolic enzyme activity confirmed that glycolytic capacity scaled positively in deep white muscle (regression slope, b=0.1 to 0.8) over a body mass range of ~20–1500 g, but only creatine phosphokinase showed positive scaling in lateral red muscle (b=0.5). Although oxidative enzymes showed negative allometry in red muscle (b=–0.01 to –0.02), mass-specific myoglobin content scaled positively (b=0.7). Capillary to fibre ratio of red muscle was higher in larger (1.42±0.15) than smaller (1.20±0.15) fish, suggesting progressive angiogenesis. By contrast, capillary density decreased (1989±161 *vs* 2962±305 mm^{-2}) as a result of larger fibre size (658±31 *vs* 307±24 μm^2 in 1595 g and 22.9 g fish, respectively). Thus, facilitated and convective delivery of O_2 show opposite allometric trends. Relative mitochondrial content of red muscle (an index of O_2 demand) varied little with body mass overall, but declined from ~40% fibre volume in the smallest to ~30% in the largest fish. However, total content per fibre increased, suggesting that mitochondrial biogenesis supported aerobic capacity during fibre growth. Heterogeneous fibre size indicates both hypertrophic and hyperplastic growth, although positive scaling of fibre myofibrillar content (b=0.085) may enhance specific force generation in larger fish. Modelling intracellular P_{O_2} distribution suggests such integrated structural modifications are required to maintain adequate oxygen delivery (calculated P_{O_2} 5.15±0.02 kPa and 5.21±0.01 kPa in small and large fish, respectively).

Key words: enzyme activity, capillaries, oxygen tension, mitochondria, red muscle, fish.

INTRODUCTION

Numerous studies have shown that biological processes, from metabolic enzyme activity to O_2 consumption of an animal, scale with body mass, for organisms of greatly differing maximum size and species relatedness (Burness et al., 1999; West et al., 2002). Structural and functional characteristics of the cardiovascular system also scale with body mass (Schmidt-Nielsen, 1984), although both aspects are rarely examined in a single study. Cells are thought to be as small as possible, commensurate with their function, in order to minimise O_2 and metabolite diffusion distances, e.g. aerobic skeletal muscle fibres used for sustained locomotion tend to be smaller than anaerobic fibres used for ballistic activity. Such scaling effects are known to be one of the most influential factors defining metabolic rate (Schmidt-Nielsen, 1984). However, muscle fine structure may also be remodelled during ontogenetic growth to augment functional capacity. Interestingly, similar changes may also occur in response to lowered environmental temperature in fishes (Egginton, 1998a), suggesting similar adaptive responses may be invoked if a metabolic error signal is derived from a mismatch in either supply or demand.

The capacity for terminal oxygen delivery represented by tissue capillarity has been measured in fish muscle using a number of different indices of varying utility (Egginton, 1992) and shown to be responsive to exercise (Sänger, 1992), cold acclimation (Egginton and Sidell, 1989) and seasonal temperature acclimatisation (Egginton and Cordiner, 1997). However, little is known of the process during normal ontogenetic growth, and how it is controlled. Growth of new capillaries (angiogenesis) is thought necessary to increase oxygen supply in response to increased oxygen demand associated with physiological challenges and during development (Hudlická et al., 1992). It is probable that the mechanisms involved include either local biochemical cues such as growth factor release, or mechanical factors such as elevated shear stress (Egginton, 2002). Changes in the microcirculation are often paralleled by changes in muscle fine structure, such as mitochondrial volume density, appearing to optimise the balance between oxygen supply and demand (Weibel et al., 1996). In addition, fibre hypertrophy (increased size) and hyperplasia (increased number) may accompany angiogenesis, and such remodelling of the host tissue can affect the distribution of blood vessels. For example, hypertrophy will increase intramuscular diffusion distances, with a proportional decline in oxygen tension within individual muscle fibres (Egginton, 1998), but the heterogeneity of capillary supply (i.e. variance of intercapillary distances) appears to be preserved irrespective of body mass by an adaptive angiogenic response (Degens et al., 2006).

Many studies have determined the interspecific allometric response of basal metabolic rate (BMR), and most recent studies agree that in mammals oxygen demand is proportional to body mass$^{2/3}$ (White and Seymour, 2005). Also of interest is the scaling exponent for structural and biochemical determinants of oxygen supply and demand in locomotory muscle, as this probably underlies an animals' behavioural repertoire. A complementary effect of organism size on indices of oxygen supply to that observed with BMR has been demonstrated in mammals (Hoppeler et al., 1981; West et al., 1997). However, there have been few estimates of the allometric response of oxygen supply in fish, the only studies known

to the authors being on the relatively sluggish eels (Egginton, 1992) and tilapia (Kisia and Hughes, 1992). By contrast, the allometric relationships among enzymes of intermediary metabolism in skeletal muscle have been studied in a number of fish species. Somero and Childress (Somero and Childress, 1980) proposed a positive allometry for glycolytic and a negative allometry for oxidative enzymes, which was subsequently confirmed in other species (Garenc et al., 1999; Norton et al., 2000; Walsh et al., 1989).

The present study provides the first integrative analysis of scaling in the structural limits to oxygen supply and demand, coupled with the metabolic profile of skeletal muscle, using a highly active fish species where these may be expected to limit locomotory performance. A mathematical model was used to predict changes in oxygen tension across red muscle fibres of average composition as a consequence of ontogenetic growth, and to explore the relative importance of different elements to this response.

MATERIALS AND METHODS

Experimental animals and tissue collection

Eleven striped bass (*Morone saxatilis* Walbaum) were sampled, over a range of body mass (BM) between 22.9 g and 1595 g. This is an active species, migrating up the Eastern seaboard of the USA, which displays impressive muscle plasticity in the face of changing environmental temperature (Sidell and Moerland, 1989). Fish were held at the University of Maine under controlled photoperiod (12 h:12 h light:dark) in filtered, aerated tap water and kept at 15±1°C for a minimum of 4 weeks before sampling. Fish were killed by a blow to the head and severing the spinal cord. A strip of slow oxidative muscle from the hypaxial lateral line triangle just posterior to the first dorsal fin, and samples of fast glycolytic (white) muscle close to the spinal column at the same position were carefully dissected.

Biochemical assays

Measurements of maximal activities of phosphofructokinase (PFK) and cytochrome oxidase (COX) were performed on fresh tissue shortly after dissection. Tissue used in measuring the maximal activities of citrate synthase (CS), pyruvate kinase (PK) and lactate dehydrogenase (LDH) were quickly frozen in liquid nitrogen and stored at –70°C until assayed. Tissue was homogenised in a 10% w/v ice-cold buffer (40 mmol l^{-1} Hepes, 1 mmol l^{-1} EDTA, 2 mmol l^{-1} $MgCl_2$, pH 7.8 at 15°C), except for tissues used for COX analysis (see below). Tissue was first minced on a chilled stage, then homogenised with two 10–15 s bursts with a Tekmar Tissuemizer, keeping the homogenate on ice between bursts. Homogenisation was completed by hand using a Tenbroeckground glass homogeniser. Dithiothreitol (DTT) was added (final concentration of 2 mmol l^{-1}) for PFK and LDH assays. Background activities were measured in the absence of initiating substrate and subtracted from total activity in the presence of substrate. Maximal activities were determined using a thermostatted cuvette carrier-equipped spectrophotometer (Perkin-Elmer Lambda 6) by measuring the rate of oxidation or reduction of pyridine nucleotides at 340 nm for 5 min, except when noted differently, with assays performed in triplicate at 15±0.5°C. Details of assay conditions are described below, following modification from original protocols (Egginton, 1986b; Norton et al., 2000), including the composition of the final reaction mixture, and the substrate/cofactor added to initiate the reaction.

Phosphofructokinase (PFK; EC 2.7.1.11): 7 mmol l^{-1} $MgCl_2$, 200 mmol l^{-1} KCl, 1 mmol l^{-1} KCN, 2 mmol l^{-1} AMP, 0.15 mmol l^{-1} NADH, 2 i.u. ml^{-1} aldolase, 10 i.u. ml^{-1} triosephosphate isomerase, 2 i.u. ml^{-1} glycerol-3-phosphate dehydrogenase, 75 mmol l^{-1} triethanolamine, pH 8.4 at 15°C; initiated by 2 mmol l^{-1} ATP + 4 mmol l^{-1} fructose 6-phosphate.

Lactate dehydrogenase (LDH; EC 1.1.1.27): 0.15 mmol l^{-1} NADH, 1 mmol l^{-1} KCN, 50 mmol l^{-1} imidazole, pH 7.7; initiated by 5 mmol l^{-1} pyruvate.

Pyruvate kinase (PK; EC 2.7.1.40): 150 mmol l^{-1} KCl, 1 mmol l^{-1} KCN, 10 mmol l^{-1} $MgSO_4$, 0.15 mmol l^{-1} NADH, 5 mmol l^{-1} ADP, 10 i.u. ml^{-1} LDH, 50 mmol l^{-1} imidazole, pH 7.1; initiated by 2.5 mmol l^{-1} phosphoenol pyruvate.

Creatine phosphokinase (CPK, EC 2.7.3.2): 10 mmol l^{-1} $MgCl_2$, 20 mmol l^{-1} glucose, 10 mmol l^{-1} *N*-acetyl-cysteine, 1 mmol l^{-1} ADP, 10 mmol l^{-1} AMP, 0.7 mmol l^{-1} $NADP^+$, 1 i.u. ml^{-1} hexokinase, 1 i.u. ml^{-1} glucose-6-phosphate dehydrogenase, 100 mmol l^{-1} imidazole, pH 7.7; initiated by 35 mmol l^{-1} creatine phosphate.

Citrate synthase (CS, EC 4.1.3.7): 0.25 mmol l^{-1} DTNB (Ellman's reagent), 0.4 mmol l^{-1} acetyl CoA, 75 mmol l^{-1} Tris-HCl, pH 8.2; initiated by 0.5 mmol l^{-1} oxaloacetate, and monitored by production of the reduced anion of DTNB at 412 nm.

Cytochrome oxidase (COX, EC 1.9.3.1): Tissue was homogenised in 50 mmol l^{-1} KH_2PO_4/KH_2PO_4, 0.05% Triton X-100, pH 7.5. The assay medium consisted of 10 mmol l^{-1} K_2HPO_4/KH_2PO_4, 0.65% (w/v) reduced (Fe^{2+}) cytochrome *c* and 0.93 mmol l^{-1} $K_3Fe(CN)_6$; initiated by the addition of homogenate and measured by oxidation of reduced cytochrome *c* at 550 nm.

Myoglobin: homogenates (10–15% w/v) were prepared using 2 mmol l^{-1} DTT, 50 mmol l^{-1} phosphate buffer, pH 7.4, sonicated 2× 5 s, and supernatants from high-speed (10,000 ***g***) centrifugation were taken for analysis. Spectrophotometric scans were taken between 620 and 490 nm, including the oxymyoglobin peaks at 581 and 543 nm, and absorbance calculated with baseline (nonspecific absorbance) subtracted. Overestimation of myoglobin content, because of contamination by haemoglobin, was estimated by gel permeation chromatography of red muscle homogenates, using a BioGel (BioRad, Hercules, CA, USA) P-100 (15 mm×280 mm) column equilibrated with 1 mmol l^{-1} DTT, 5 mmol l^{-1} EDTA, 50 mmol l^{-1} Tris pH 7.6 at 5°C. Concentrations were calculated from pooled fractions, using 4 cm path length cuvettes, and millimolar extinction coefficients of εmM 581=14.6 and εmM 543=13.6 (Egginton, 1986b).

Muscle fixation

Samples were pinned at resting length on strengthened cork and immersed in a fixative consisting of 1% glutaraldehyde, 4% formaldehyde, 0.1 mol l^{-1} phosphate buffer, 10% sucrose and 0.2% $CaCl_2$ (pH 7.3 and vehicle osmolality 482 mOsm), then post-fixed in buffered 1% osmium tetroxide (Egginton and Cordiner, 1997; Egginton and Sidell, 1989). Two to four blocks were prepared per fish, and one chosen at random for examination. For light microscopy, semi-thin (0.5 μm) sections were cut and stained with 1% Toluidine Blue, then viewed under an Olympus BH-2 microscope with a drawing arm. For transmission electron microscopy, ultra-thin (~80 nm) sections were cut and mounted on Formvar-coated copper grids, stained with 30% uranyl acetate and Reynold's lead citrate, then viewed under a Jeol 1200 electron microscope at an accelerating voltage of 60 kV.

Morphometry

Semi-thin (0.5 μm) sections were viewed at a magnification of ×500 to obtain estimates of capillary density (CD; mm^{-2}) capillary to fibre ratio (C:F) and mean fibre area ($\overline{A}_f$; μm^2) using an unbiased sampling protocol (Egginton, 1990). Digital images (×500, Zeiss

Axioskop 2 plus microscope, AxioCam MRc camera) were imported into ImageJ software (NIH, USA), individual fibres outlined to obtain area and perimeter, and fibre size distribution constructed.

The principles of stereology, an application of geometrical probability theory that permits extrapolation of structural information from n to n+1 dimensions [e.g. length to surface, area to volume (Weibel, 1979)] were used to quantify muscle fine structure from electron micrographs. Volume and surface densities represent the area and boundary length of any structure as a proportion of a reference cross-sectional area; surface to volume ratio and profile cross-sectional areas are calculated in a similar manner. A systematic random sampling regime was used to quantify muscle fine structure as volume density (V_v, volume of object per unit volume of reference; $\mu m^3 \mu m^{-3}$), surface density (S_v, surface area of object per unit volume of reference; $\mu m^2 \mu m^{-3}$), and surface to volume ratio (S/V; $\mu m^2 \mu m^{-3}$) of components relevant to oxygen delivery and consumption. Organelle content of muscle fibres was calculated as the product of volume density and fibre cross-sectional area. These results were analysed with respect to body mass using the allometric equation:

$$Y = aW^b , \quad (1)$$

where Y is the parameter examined, a is a normalisation constant (the value of y-axis intercept), W is the body mass (g) and b is the scaling exponent (slope of the regression line) (Schmidt-Nielsen, 1984). The value of b will vary among organisms with different traits, and biological processes with different characteristics, and represents the sum of multiple influences on control. For whole body traits 'positive allometry' means that the scaling slope is >1, whereas 'negative allometry' means it is <1. However, for mass-specific traits, as used here, 'positive allometry' means that the scaling slope is >0, whereas 'negative allometry' means it is <0.

To illustrate the range of response associated with differences in body mass, a minimum of 20 capillaries from each of the two smallest and two largest fish were analysed at a final magnification of ×5400 to ×12,934, to quantify microvessel structure and provide a nominal scoring of a range of angiogenic indices (Egginton et al., 2001). In addition, a montage containing 12 capillaries from each of the two smallest fish, and individual micrographs around 12 capillaries from each of the two largest fish (a montage was not possible at adequate resolution because of the lower capillary density) were taken at a magnification of ×2400. Volume density of mitochondria was calculated in four concentric annulae of equal area. The maximum radius of the outermost annulus was set at half the mean intercapillary distance, measured iteratively on the montage until a stable estimate of the mean was achieved. The median capillary radius was used as the value for the inner ring around the perimeter of the capillary (Egginton and Sidell, 1989).

Mathematical modelling

The dimensionless Reynolds number was estimated for the smallest fish using the equation:

$$Re = (LU) / \nu , \quad (2)$$

where L is body length (116 mm for small fish), ν is the dynamic viscosity of water at 15°C (1.14 centistokes), and assuming a velocity, U, of 10 $BL\,s^{-1}$ (BL, body lengths) as a reasonable estimate of cruising speed for striped bass of that size, at that temperature (Kerr, 1953).

Capillary radius was used to estimate potential limits to microvascular blood flow ($\dot{Q}$), according to the Hagan-Poiseuille equation:

$$\dot{Q} = (\pi r^4 \mathrm{MABP}) / (8L\eta) , \quad (3)$$

where r is vessel radius (μm), MABP is the mean arterial blood pressure, L is vessel length (mm) and η is blood viscosity (cP). Although values for these are not, to our knowledge, available for striped bass, MABP in rainbow trout is 3.2 kPa (Sandblom and Axelsson, 2005) and trout blood at the same temperature has a measured viscosity of 5.4 cP (Egginton and Rankin, 1998). Capillary length is an unknown so we performed two calculations, the first assuming individual vessel L varies proportionally with myotome length, and therefore body length, and the second assuming L is a constant in all body sizes. Total capillary length would then equate to (L×CD×muscle mass). Using a published regression equation for striped bass length *vs* BM (Rodnick and Sidell, 1995), and scaling of red muscle mass in trout as a guide to that in bass (Goolish, 1989), enabled calculation of upper and lower boundaries for changes in $\dot{Q}$.

The combined effect of changes in fine structure on intracellular oxygen tension of slow muscle fibres was explored by means of a mathematical model of diffusion (Hoofd and Egginton, 1997). Briefly, the potential oxygen delivery (determined by capillary supply) is distributed according to oxygen consumption (scaled according to mitochondrial volume), allowing for the diffusion distances involved (varying with fibre size) and oxygen permeability (given by the ratio of intracellular lipid to aqueous sarcoplasm), corrected for the kinetic effects of temperature (Q_{10}), and partitioned among the distinct structural regions found in fish muscle fibres (subsarcolemmal and intermyofibrillar zones). For clarity the results are presented as wireframe three-dimensional plots.

Statistical analysis

Single-factor analysis of variance (ANOVA) was used for comparison of values, with Fisher's PLSD to estimate significance between groups. Sufficiency of sample size for stereological parameters was tested by determining the stability of population means on replicate analysis. Distribution analysis of fibre area used the Kolmogorov–Smirnow procedure and comparisons from Mann–Whitney U-tests. Data are presented as mean ± s.e.m. with number of fish (N) or observations (n) given in parentheses, as appropriate. For allometric relationships, the coefficient of determination (R^2) corresponds to the amount of variation explained by the best-fit regression line, and the F-test was used to determine whether the slope was significantly different from zero (P<0.05).

Chemicals

All chemicals were of reagent grade or better quality (BDH or Sigma, Poole, Dorset, UK). Glutaraldehyde and Araldite resin were of EM grade (Agar Scientific Ltd, Stanstead, Essex, UK).

RESULTS

Enzyme activity

In white muscle, significant scaling effects were observed in mass-specific activities of PK, LDH and PFK (b=0.110, 0.342 and 0.105, respectively). Interestingly, the glycolytic enzyme CPK displayed strong positive allometry in both white and red muscle (b=0.824 and 0.528, respectively, R^2=0.900 in both cases). The oxidative enzymes COX and CS demonstrated negative allometry in red muscle (b=–0.014 and –0.022, respectively), in contrast to the index

Table 1. Regression analysis against body mass of myoglobin concentration and enzyme activity in red and white muscle

	Equation $Y=aW^b$	Coefficient of determination (R^2)	Standard error of the slope (b)	P-value
Red muscle				
[Mb]	$759.079W^{0.745}$	0.502	0.170	0.0003
COX	$49.626W^{-0.014}$	0.503	0.004	0.0045
CS	$58.473W^{-0.022}$	0.383	0.007	0.0069
PK	$85.025W^{0.020}$	0.132	0.014	0.1837
LDH	$275.317W^{0.033}$	0.121	0.023	0.1720
PFK	$58.146W^{-0.017}$	0.163	0.009	0.0776
CPK	$49.675W^{0.528}$	0.896	0.054	<0.0001
White muscle				
[Mb]	$63.517W^{0.003}$	0.003	0.012	0.8038
COX	$1.439W^{-0.001}$	0.247	2.354×10^{-4}	0.0424
CS	$1.200W^{-3.356\times10^{-5}}$	0.003	1.693×10^{-4}	0.8462
PK	$146.786W^{0.110}$	0.451	0.022	0.0044
LDH	$509.240W^{0.342}$	0.487	0.091	0.0018
PFK	$105.833W^{0.105}$	0.547	0.023	0.0002
CPK	$156.856W^{0.824}$	0.900	0.083	<0.0001

COX, cytochrome oxidase; CS, citrate synthase; PK, pyruvate kinase; LDH, lactate dehydrogenase; PFK, phosphofructokinase; CPK, creatine phosphokinase.
Y is the parameter examined, a is a normalisation constant (the value of the y-axis intercept), W is the body mass (g) and b is the scaling exponent (slope of the regression line).
[Mb], myoglobin concentration (nmol l^{-1} g wet mass^{-1}); enzyme activity (i.u. g wet mass^{-1} min^{-1}).

of facilitated oxygen diffusion, mass-specific myoglobin content, which displayed positive allometry (b=0.745; Table 1).

Muscle histology

Representative muscle sections from large and small fish are shown in Fig. 1, illustrating the similar mitochondrial content, changes in fibre size and scaling of capillarity with body mass. Red muscle C:F increased with fish mass (R^2=0.946), but mean fibre area, $\overline{A}_f$, also increased (R^2=0.760), hence decreasing CD (R^2=0.929), with an apparent boundary between small and large size classes at 200–300 g BM (Fig. 2). A different fibre size distribution in small and large fish was evident (Fig. 3), being right-shifted in the latter (P<0.0001).

Muscle fine structure

The mitochondrial volume density of red muscle fibres, V_v(mit,f), showed little evidence for an established allometric relationship (b=–6.069×10^{-5}, R^2=0.255, n.s.; Fig. 4), reflecting the sum of changes in regional distribution for intermyofibrillar [$V_v(\text{mit}_{imf},f)$, b=–1.340×10^{-5}] and subsarcolemmal [$V_v(\text{mit}_{ss},f)$, b=–4.043×10^{-5}] populations (Table 2). There was no significant change in total mitochondrial content of fibres, V(mit,f), given as the product of V_v(mit,f) and $\overline{A}_f$ (b=0.031, R^2=0.233, n.s.; Table 3). Fibre hypertrophy associated with growth led to little change in the relative content of contractile material, V_v(myo,f). However, this was not simply a consequence of adjustments in other compartments (Fig. 4), as the product of V_v(myo,f) and $\overline{A}_f$ showed significant positive scaling (b=0.085, R^2=0.799, P=0.001). Nuclei and intracellular lipid droplets occupied a constant, low proportion of muscle fibres (Table 3).

The extracellular space of red muscle showed a modest negative scaling response (b=–2.923×10^{-5}, R^2=0.561, P=0.020; Fig. 4), showing closer packing of fibres in large fish. Conversely, positive scaling was found for the volume of sarcoplasm in the intermyofibrillar zone (b=5.245×10^{-5}, R^2=0.819, P<0.001), although no significant relationship was found in the subsarcolemmal zone of muscle fibres (b=1.641×10^{-5}, R^2=0.112).

V_v(mit,f) decreased with increasing distance from the point of oxygen supply (capillary) in both large and small fish, when normalised as a percentage of the intercapillary distance (ICD), with the outer radius being 47% of the maximal ICD. In large fish there

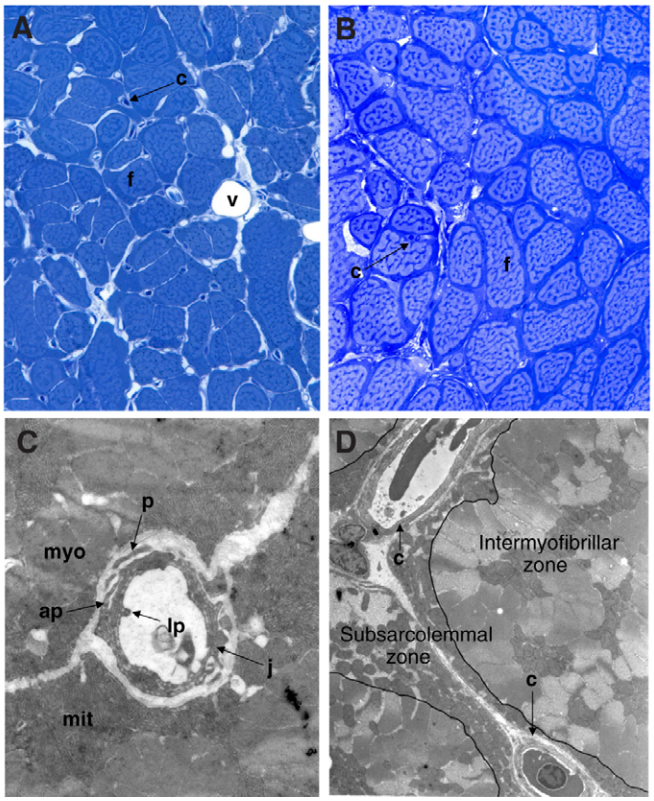

Fig. 1. Cross-sections of muscle stained with Toluidine Blue, (A) from a small fish viewed at ×500 original magnification showing numerous capillaries (c) and many small fibres (f; v, venule) and (B) from a large fish viewed at ×500 original magnification, showing fewer capillaries (c) and larger muscle fibres (f). Note the heterogeneity in fibre size distribution indicative of both hypertrophy and hyperplasia during growth. (C) TEM images showing detail of an individual capillary from a small fish at ×8640 original magnification, showing a junction between endothelial cells in the capillary wall (j), and both lumenal (lp) and ablumenal processes (ap). A pericyte (p) is in close association with the capillary. Myofibrils (myo) and mitochondria (mit) from the surrounding muscle fibre are also evident. (D) TEM image of muscle fibres from large fish at ×3600 original magnification, showing division of fibre into intermyofibrillar and subsarcolemmal zones. Also present are two capillaries (c).

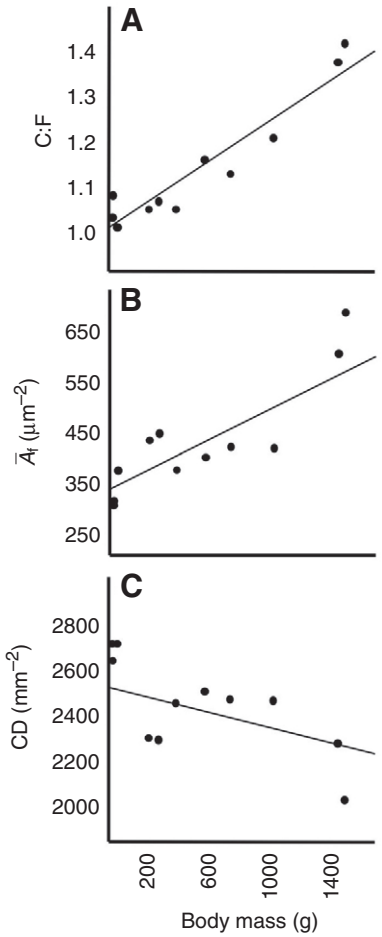

Fig. 2. Angiogenesis compensates for muscle fibre growth. (A) Regression of capillary to fibre ratio (C:F) against mass, Y=0.991$W^{2.328-4}$, R^2=0.904. (B) Regression of $\bar{A}_f$ against mass, Y=313.6$W^{0.166}$, R^2=0.760. (C) Regression of capillary density (CD) against mass, Y=2585.9$W^{-0.27}$, R^2=0.533.

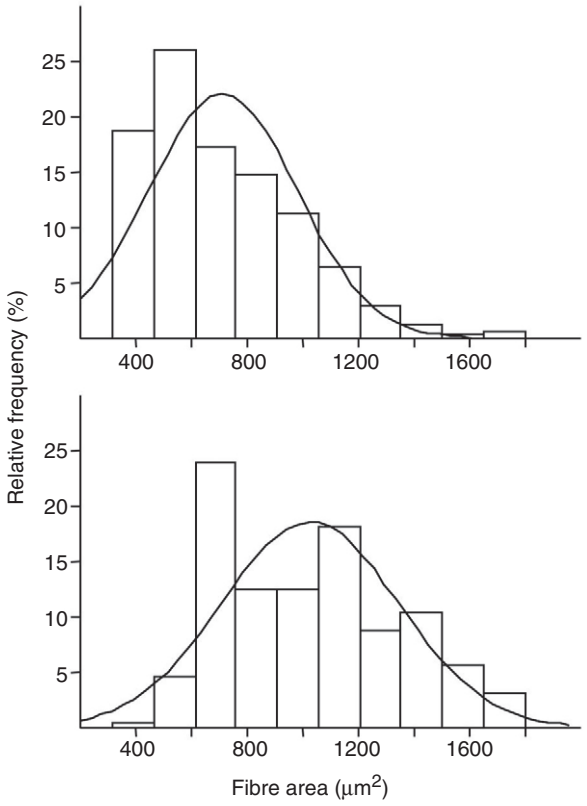

Fig. 3. Relative fibre size distribution (%) in small (top) and large fish (bottom), P<0.0001 (Mann–Whitney U-test). Mean fibre size=826.04±18.72 μm^2 (large) *vs* 512.97±10.94 μm^2 (small).

was a significant decrease in V_v(mit,f) as the ICD is approached (P<0.05), whereas for the smaller fish the reduction in radial distribution of mitochondria was more variable (n.s.), although at any relative distance from a capillary V_v(mit,f) was greater in the small than the large fish (Fig. 5). Consistent with the global analysis of muscle fine structure total mitochondrial content, given as the product of V_v(mit,f) and $\bar{A}_f$, was greater in large than small fish (464±23 and 222±7 μm^2, respectively; P<0.01).

Capillary fine structure

The lumen occupied a larger proportion of the capillary cross-sectional area during ontogenetic growth, following the trend for greater capillary area and lower S/V with increasing BM (Table 4). Other structural parameters known to vary with metabolic status showed little differences among the size classes (Table 4), and there were no significant differences in any of the angiogenic indices measured (Table 5). Consequently, estimates of theoretical maximum blood flow, $\dot{Q}$ (relative units), for individual vessels showed no significant difference between small and large fish under the boundary conditions that L does not vary with body size (small fish $\dot{Q}$=2.362±0.123, large fish $\dot{Q}$=2.062±0.038), or that it is reduced sixfold if L varies with body length ($\dot{Q}$=2.062±0.141 and 0.383±0.010, respectively). Allowing for changes in capillary size, CD and red muscle mass, then microvascular volume in large fish is probably about fourfold greater than that in small fish, and with a similar MABP then the difference in $\dot{Q}$ would be at least as great.

Intracellular oxygen tension

Estimates of P_{O_2} across a red muscle fibre of average composition suggest that oxygen tension is maintained during ontogenetic growth (mean P_{O_2}=5.148±0.016 kPa and 5.209±0.010 kPa for the smallest and largest fish, respectively). We used 'in silico' analysis to explore the consequences of not undertaking the observed tissue remodelling. If fibre size varied inversely with body mass (i.e. hyperplasia rather than hypertrophy dominated) but all other influences were the same, then small fish modelled with fibre area appropriate for large fish show a reduced mean P_{O_2} (3.791±0.024 kPa) as well as lower minimum P_{O_2} (3.19 kPa *vs* 4.86 kPa with normal fibre size), whereas complementary changes applied to large fish made little difference to mean or minimum P_{O_2} (Fig. 6). Reversing the scaling of capillary cross-sectional area had a minor effect in fibres from small fish (mean P_{O_2} increased to 5.263±0.015 kPa, minimum=4.97 kPa) or from large fish (mean P_{O_2} decreased to 5.084±0.011 kPa, minimum=4.84 kPa). However, a greater effect was seen by changing the number of capillaries around a fibre, with fibres from small fish modelled with capillary supply appropriate for large fish having a higher calculated mean and minimum P_{O_2} (5.544±0.009 and 5.39 kPa, respectively). A reduction in mean P_{O_2} to 4.559±0.018 kPa was calculated for a representative fibre from a large fish having the capillary supply of small fish, with the minimum P_{O_2} reducing to 4.12 kPa. As there was very little difference in mitochondrial density between the two

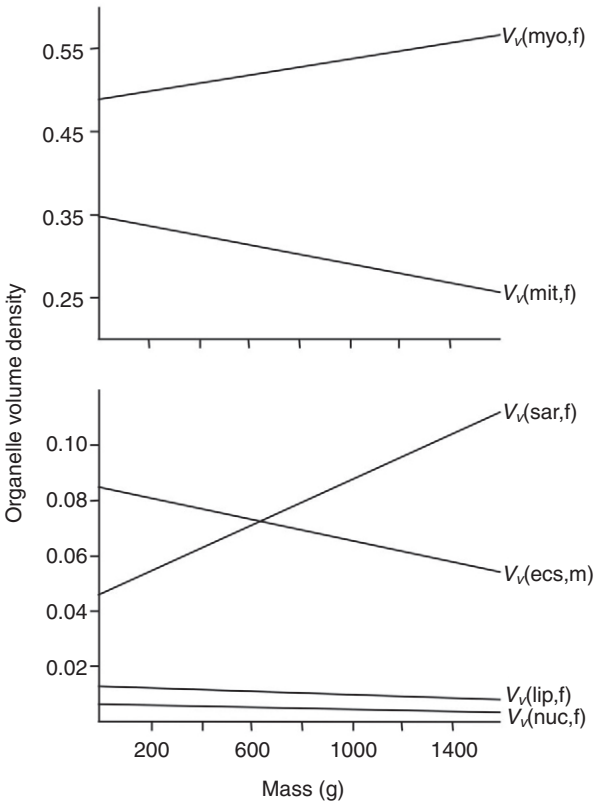

Fig. 4. Changes in organelle volume density of red muscle fibres with body mass. Linear regressions are: V_v(myo,f)=0.489+4.921$^{-5}\times M$, R^2=0.159; V_v(mit,f)=0.346–5.587$^{-5}\times M$, R^2=0.242; V_v(sar,f)=0.047 + 4.098$^{-5}\times M$, R^2=0.384; V_v(ecs,m)=0.085–1.939$^{-5}\times M$, R^2=0.441; V_v(lip,f)=0.013–2.908$^{-6}\times M$, R^2=0.031; V_v(nuc,f)=0.007–1.701$^{-6}\times M$, R^2=0.043. ecs, extracellular space; f, fibre; l, lipid; m, muscle; mit, mitochondria; myo, myofibrils; nuc, nucleus; sar, sarcoplasm.

groups, the effects of reversing this were trivial, suggesting tight regulatory control.

DISCUSSION

Scaling considerations

The hydrodynamics of swimming in small organisms may be influenced by fluid viscosity. However, Reynolds number estimated for the smallest fish, Re=1.1×10^{-5}, is well above the threshold for swimming to be affected by the inertial rather than the viscous regime, calculated to be around Re=300. Hence, even the smallest fish in the present study would be unaffected by the viscous effects of water (McHenry and Lauder, 2005). The present study also avoids really large fish where scaling effects appear to wane (Norton et al., 2000) such that the size range studied, spanning two orders of magnitude in body mass, appears to be optimal to explore the integrative nature of any ontogenetic scaling response.

Many recent studies have shown that the metabolic scaling exponent varies substantially among vertebrates, mostly between 2/3 and 1 (e.g. Glazier, 2005; White et al., 2006). Oxygen consumption has been reported to scale with an exponent of 0.793 in a survey of 69 fish species (Clarke and Johnston, 1999). However, this reflects a range of ~0.4–1.3 among species, with little obvious correlation with lifestyle or body form. Unfortunately, comparable data on scaling of $\dot{M}_{O_2}$ in striped bass are not available, although estimates of particular sized fish confirm that this is one of the more aerobic species, e.g. 150 mg O_2 h^{-1} kg^{-1} for 50–75 g striped bass at 15°C [assuming an exponent of 2/3 (Mitchell and Cech, 1994)]. In many vertebrates there is a non-linear (Type III) ontogenetic shift in scaling exponent, from isometric (b=1) in larval stages to negative allometry (b<1) in juveniles and adults (Bochdansky and Leggett, 2001). Such data do not exist for striped bass, but in spotted seatrout (*Cynoscion nebulosus*), which has a similar body form, a break in the allometric relationship occurs at 480 μg dry mass (~2.4 g wet mass), from b=1.04 to b=0.78 (Wuenschel et al., 2004). All the fish sampled in the present study may therefore be expected to lie on the same allometric curve.

The allometric dependence of metabolic rate on body size continues to be a controversial subject. Organisms exhibiting scaling exponents close to 3/4 for metabolic rate and close to 1/4

Table 2. Regression against body mass of red muscle organelle volume density and surface density

	Equation $Y=aW^b$	Coefficient of determination (R^2)	Standard error of the slope (b)	P-value
V_v(myo,f)	0.007W$^{-4.561\times10^{-6}}$	0.307	2.589×10^{-6}	0.6810
V_v(nuc,f)	0.489W$^{2.272\times10^{-6}}$	0.026	5.299×10^{-5}	0.1215
V_v(mit$_{imf}$,f)	0.156W$^{-1.340\times10^{-5}}$	0.053	2.145×10^{-5}	0.5520
V_v(mit$_{ss}$,f)	0.196W$^{-4.043\times10^{-5}}$	0.281	2.444×10^{-5}	0.1421
V_v(mit,f)	0.356W$^{-6.069\times10^{-5}}$	0.255	3.918×10^{-5}	0.1653
V_v(lip$_{imf}$,f)	0.003W$^{4.107\times10^{-6}}$	0.131	3.996×10^{-6}	0.3383
V_v(lip$_{ss}$,f)	0.003W$^{1.213\times10^{-6}}$	0.024	2.915×10^{-6}	0.6897
V_v(lip,f)	0.009W$^{5.301\times10^{-7}}$	0.001	6.217×10^{-6}	0.9344
V_v(ecs,m)	0.095W$^{-2.923\times10^{-5}}$	0.561	9.775×10^{-5}	0.0202
V_v(sar$_{imf}$,f)	0.003W$^{5.245\times10^{-5}}$	0.819	9.314×10^{-6}	0.0008
V_v(sar$_{ss}$,f)	0.039W$^{1.641\times10^{-5}}$	0.112	1.746×10^{-5}	0.3787
V_v(sar,f)	0.040W$^{6.892\times10^{-5}}$	0.614	2.066×10^{-5}	0.0125
S_v(mit$_{imf}$,f)	0.663W$^{-6.256\times10^{-5}}$	0.087	7.659×10^{-5}	0.4409
S_v(mit$_{ss}$,f)	0.756W$^{-9.843\times10^{-5}}$	0.144	9.070×10^{-5}	0.3138
S_v(mit,f)	1.419W$^{-1.610x\times10^{-4}}$	0.138	1.519×10^{-4}	0.3243
S_v(lip$_{imf}$,f)	0.029W$^{1.810\times10^{-5}}$	0.002	1.635×10^{-5}	0.9150
S_v(lip$_{ss}$,f)	0.031W$^{-1.125\times10^{-5}}$	0.094	1.321×10^{-5}	0.4226
S_v(lip,f)	0.060W$^{-1.306\times10^{-5}}$	0.025	2.890×10^{-5}	0.6651

V_v, organelle volume density; S_v, surface density; myo, myofibrils; f, fibre; nuc, nucleus; mit, mitochondria; imf, intermyofibrillar; ss, subsarcolemmal; lip, lipid; ecs, extracellular space; m, muscle; sar, sarcoplasm.

Y is the parameter examined, a is a normalisation constant (the value of the y-axis intercept), W is the body mass (g) and b is the scaling exponent (slope of the regression line).

Table 3. Regression against body mass of organelle volume and surface area in red muscle fibres

	Equation $Y=aW^b$	Coefficient of determination (R^2)	Standard error of the slope (b)	P-value
V(myo,f)	$160.450W^{0.085}$	0.799	0.016	0.0012
V(nuc,f)	$3.162W^{-0.009}$	0.081	0.001	0.4585
$V(mit_{imf},f)$	$51.308W^{0.016}$	0.308	0.009	0.1208
$V(mit_{ss},f)$	$58.203W^{0.018}$	0.250	0.012	0.1704
V(mit,f)	$113.610W^{0.031}$	0.233	0.021	0.1878
$V(lip_{imf},f)$	$1.397W^{0.002}$	0.148	0.001	0.3059
$V(lip_{ss},f)$	$0.940W^{0.001}$	0.150	0.001	0.3033
V(lip,f)	$2.339W^{0.003}$	0.160	0.002	0.2865
$V(sar_{imf},f)$	$-2.589W^{0.034}$	0.762	0.007	0.0021
$V(sar_{ss},f)$	$13.197W^{0.015}$	0.343	0.008	0.0973
V(sar,f)	$10.607W^{0.049}$	0.672	0.013	0.0068
$S(mit_{imf},f)$	$214.442W^{0.078}$	0.378	0.038	0.0778
$S(mit_{ss},f)$	$247.287W^{0.074}$	0.228	0.051	0.1934
S(mit,f)	$461.731W^{0.151}$	0.314	0.0084	0.1164
$S(lip_{imf},f)$	$8.449W^{0.005}$	0.078	0.006	0.4665
$S(lip_{ss},f)$	$9.653W^{-1.598\times10^{-4}}$	1.544×10^{-4}	0.005	0.9747
S(lip,f)	$18.107W^{0.005}$	0.025	0.011	0.6843

V, organelle volume; S, surface area.
Y is the parameter examined, a is a normalisation constant (the value of the y-axis intercept), W is the body mass (g) and b is the scaling exponent (slope of the regression line).
NB: $V=V_v\times\bar{A}_f=\mu m^3\,\mu m^{-3}\times\mu m^2=\mu m^2$; $S=S_v\times\bar{A}_f=\mu m^2.\mu m^{-3}\times\mu m^2=\mu m$.

for internal times and distances, represent the theoretical maximal and minimal values for the effective surface area and linear dimensions for a volume-filling, fractal-like hierarchical branching vascular networks, respectively (West et al., 1999; White et al., 2007), suggesting that supply rates determine metabolic rates. However, the metabolic rate of isolated cells also declines with increasing body mass. In addition, the scaling exponent characterises the relationship between body mass and basal (resting) metabolic rate, when elements of the oxygen delivery pathway may be expected to display excess capacity. Another approach would therefore be to adopt a multiple-causes model of allometry (Suarez and Darveau, 2005), based on metabolic control theory that identifies multiple contributors to metabolic rate. This may be especially important at sub-maximal rates, but as the relevant input data are not available one may use maximal enzyme capacity as an index of potential energy flux through different pathways, with suitable caution. For oxygen supply and demand the situation is a little easier, since structure can only identify capacities, and substrate supply plays an increasing role in limiting whole animal $\dot{M}_{O_2}$. Therefore, the values for b in this study may be expected to differ from that for basal $\dot{M}_{O_2}$, and may better reflect $\dot{M}_{O2max}$.

Finally, in a field where statistical significance is treated as essential to discussion about the possible mechanistic basis of scaling responses, we caution that this is not always helpful. Recall that $P<0.05$ is a value adopted by convention, but lacking any theoretical foundation, its biological relevance depending on both importance of the process (cf. blood pH *vs* body mass) and whether a parameter is viewed in isolation (cf. overall oxygen delivery and demand). The flux of oxygen is part of a cascade of events, each of which involves a resistance and capacitance term. Small differences in one element may still give rise to functionally important effects because of the multiplicative response of the system as a whole. We have previously shown this to be the case with thermal acclimatisation (Egginton et al., 2000) where between any two seasons a single morphometric parameter was difficult to identify as statistically significant, however, the integrated response was clearly season dependent. The negative scaling relationship in specific mitochondrial content we identify, with suitable caveats, as probably being important must be viewed as part of the integrative whole, e.g. these structural data are consistent with an independent estimate of oxidative capacity, that of enzyme activity.

Metabolism

Most studies on scaling of metabolic enzymes in fish have concentrated on white muscle because of its functional significance in rapid movements to avoid predation or capture food. The anaerobic enzymes PK and/or LDH showed a positive scaling exponent for mass-specific activity, potentially enabling a greater burst swimming performance in larger fish, with anaerobic enzymes in red muscle also contributing to power output (Somero and Childress, 1980). This interpretation was supported by a lack of scaling in inactive fish (Goolish, 1991) and in tissue not involved in locomotion (Childress and Somero, 1990). Subsequent studies have confirmed this general pattern, although interspecific differences are influenced by life history, activity levels and

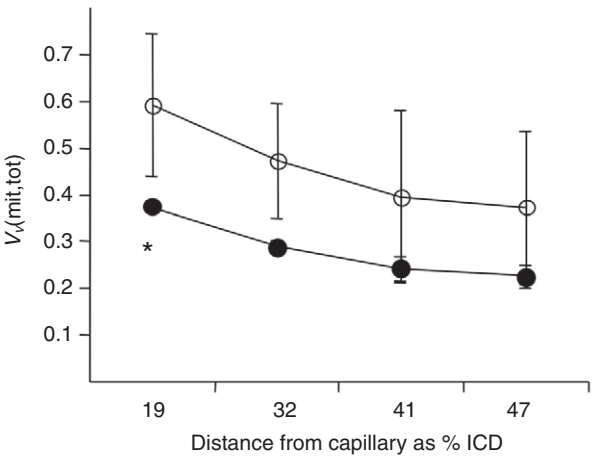

Fig. 5. Changes in mean V_v(mit,f) with increasing distance from a capillary in large (filled circles) and small fish (open circles). Error bars indicate ±s.d.; *mitochondrial content closest to capillaries is significantly different from the perivascular region in red muscle of large fish at 32% (P=0.033), 41% (P=0.008) and 47% intercapillary distance, ICD (P=0.006).

Table 4. Capillary structure and pericyte coverage in small and large fish

	Small fish	Large fish
V_v(cyt,ec)	0.460±0.040	0.380±0.020
V_v(nuc,ec)	0.050±0.010	0.040±0.010
V_v(lum,cap)	0.490±0.050	0.585±0.035
S_v(lum,cap) μm^{-1}	1.495±0.125	1.325±0.085
S_v(ec,cap) μm^{-1}	1.815±0.155	1.480±0.070
S/V(lum) μm^{-1}	3.405±0.595	2.590±0.240
S/V(cap) μm^{-1}	4.225±0.645	2.295±0.185
S/V(peri,cap) μm^{-1}	2.625±0.175	0.890±0.610
$\bar{A}$(cap) μm^2	10.010±2.860	15.075±0.105
Peri. coverage	0.285±0.005	0.190±0.130

V_v, organelle volume density; S_v, surface density; cyt, cytoplasm; ec, endothelial cell; nuc, nucleus; cap, capillary; lum, lumen; peri, pericyte; $\bar{A}$, mean area. Values are means±s.d.

Table 5. Nominal scoring of angiogenic variables in capillaries from small and large fish

	Small fish	Large fish
Number of lumenal processes	2.47±0.35	2.28±0.48
Junctional lumenal processes	0.87±0.17	0.78±0.16
Non-junctional lumenal processes	1.6±0.19	1.53±0.34
Number of ablumenal processes	1.83±0.59	1.57±0.59
Junctional ablumenal processes	0.7±0.14	0.42±0.17
Non-junctional ablumenal processes	1.13±0.46	1.21±0.44
Pericyte number	2.44±0.22	1.55±0.51
Junctional pericytes	0.72±0.09	0.34±0.08
Non-junctional pericytes	1.73±0.21	1.21±0.47
Fibroblast number	0.44±0.11	0.33±0.15

Values are means±s.d. of score per capillary.

phylogenetic relationships (Childress and Somero, 1990). Hence, LDH and PK showed positive allometry (b>0) in white muscle of many fishes (Burness et al., 1999; Davies and Moyes, 2007; Ewart et al., 1988; Martinez et al., 2000; Sullivan and Somero, 1983; Torres and Somero, 1988), whereas in striped bass positive scaling was found in small and medium, but not large (>1000 g) fish (Norton et al., 2000). The same trend was also demonstrated in the present study in which LDH scaled with a similar exponent (b=0.342) to that previously reported (b=0.31) (Norton et al., 2000), although PK had weaker positive allometry (b=0.110 and b=0.56, respectively). The different size ranges examined and sample sizes may explain this discrepancy, hence the overall scaling pattern may be weakened by values from larger fish. Although these enzymes may provide an index of sustained glycolytic capacity, whether or not they are rate-limiting, a better guide to burst activity may be derived from the capacity to re-phosphorylate the high-energy reservoir of phosphocreatine. Importantly, CPK also displayed positive allometry in trout white muscle (Burness et al., 1999) and in the present study, where the scaling exponent showed the strongest positive allometry (P<0.0001). By contrast, the oxidative enzymes COX and CS displayed negative allometry in fish white muscle (Davies and Moyes, 2007; Martinez et al., 2000; Torres and Somero, 1988; Tripathi and Verma, 2004). However, CS displayed no size dependence in other species (Burness et al., 1999; Torres and Somero, 1988). Again, such intraspecific differences in scaling may be attributed to variations in lifestyle (Sänger, 1993), activity level (Burness et al., 1999) as well as diet, season and latitude (Sullivan and Somero, 1983). No size-dependence in COX or CS was found in white muscle in the present study, as previously reported for striped bass (Norton et al., 2000), suggesting recovery from exercise was not compromised by size.

There have been fewer studies on scaling of metabolic enzymes in fish red muscle. Importantly, this may provide an index of aerobic capacity during routine swimming, which for many species represents the majority of locomotory activity. In striped bass red muscle oxidative enzymes (CS and malate dehydrogenase, MDH) showed size independence, whereas glycolytic enzymes in the smallest size class had similar activity and positive scaling in both red and white muscle, suggesting that red muscle may contribute to anaerobic performance in small, but not large fish (Norton et al., 2000). Whether that reflects the poor differentiation among muscle type at that stage is unclear. In the present study, the only glycolytic enzyme to display significant scaling in red muscle was CPK, supporting the idea that in striped bass the red muscle may contribute to re-phosphorylation of phosphocreatine during burst swimming of larger fish. Consistent with this pattern is reduced activity of the oxidative enzymes, COX and CS, with increasing body mass.

Thus, the metabolic potential of skeletal muscle differs according to the requirement for O_2, with the general size independence of aerobic enzyme activity suggesting a limitation met by positive scaling of glycolytic enzymes. Interestingly, there may be differential control of these responses, involving transcriptional regulation of anaerobic and post-translational regulation of aerobic enzyme activity (Davies and Moyes, 2007). In addition to enzymatic activity, aerobic capacity may also be determined by the structural limits to oxygen supply and demand (below). Indeed, there is compelling evidence that oxygen delivery is a limiting factor in aerobic metabolism with increasing cell size (Pörtner, 2002).

A decrease in activity of enzymes used in aerobic respiration with increasing body size is to be expected as mass-specific oxygen demand is inversely related to BM, and scaling patterns in aerobic enzymes may therefore be determined by capacity for oxygen transport (Schmidt-Nielsen, 1984). Enzyme activities are estimated under optimal conditions, so it is necessary to examine other aspects of the O_2 delivery cascade to determine whether such capacity may be realised *in vivo*. Myoglobin concentration, [Mb], was found to be independent of size in white and cardiac muscle of sea raven (Ewart et al., 1988), a sluggish sculpin-like species, whereas cardiac [Mb] increased with body size in more active species such as tuna (Poupa et al., 1981) and salmonids (Ewart and Driedzic, 1987). These data indicate a positive scaling of facilitated O_2 diffusion in species with high aerobic enzyme capacity, as influenced by activity levels. This is supported by our data showing no allometric influence in white muscle (b=0.003) but positive scaling (b=0.745) in red muscle of a migratory piscivore, suggesting that decreased oxidative capacity is not a consequence of impaired facilitated O_2 diffusion. To assess whether structural determinants of O_2 supply and demand complemented these changes, we quantified the mitochondrial content and capillarity of red muscle.

Mitochondria

According to theory, natural selection may optimise both metabolic capacity and intracellular efficiency, by maximising the scaling of exchange surface areas and minimising the scaling of transport distances and times, respectively (West et al., 1999). However, as short diffusion distances facilitate rapid O_2 flux to mitochondria and ATP flux to sites of demand, a large fibre size will probably reduce the aerobic capacity (Kinsey et al., 2007). Mitochondrial biogenesis accompanied growth in eel (Egginton and Johnston,

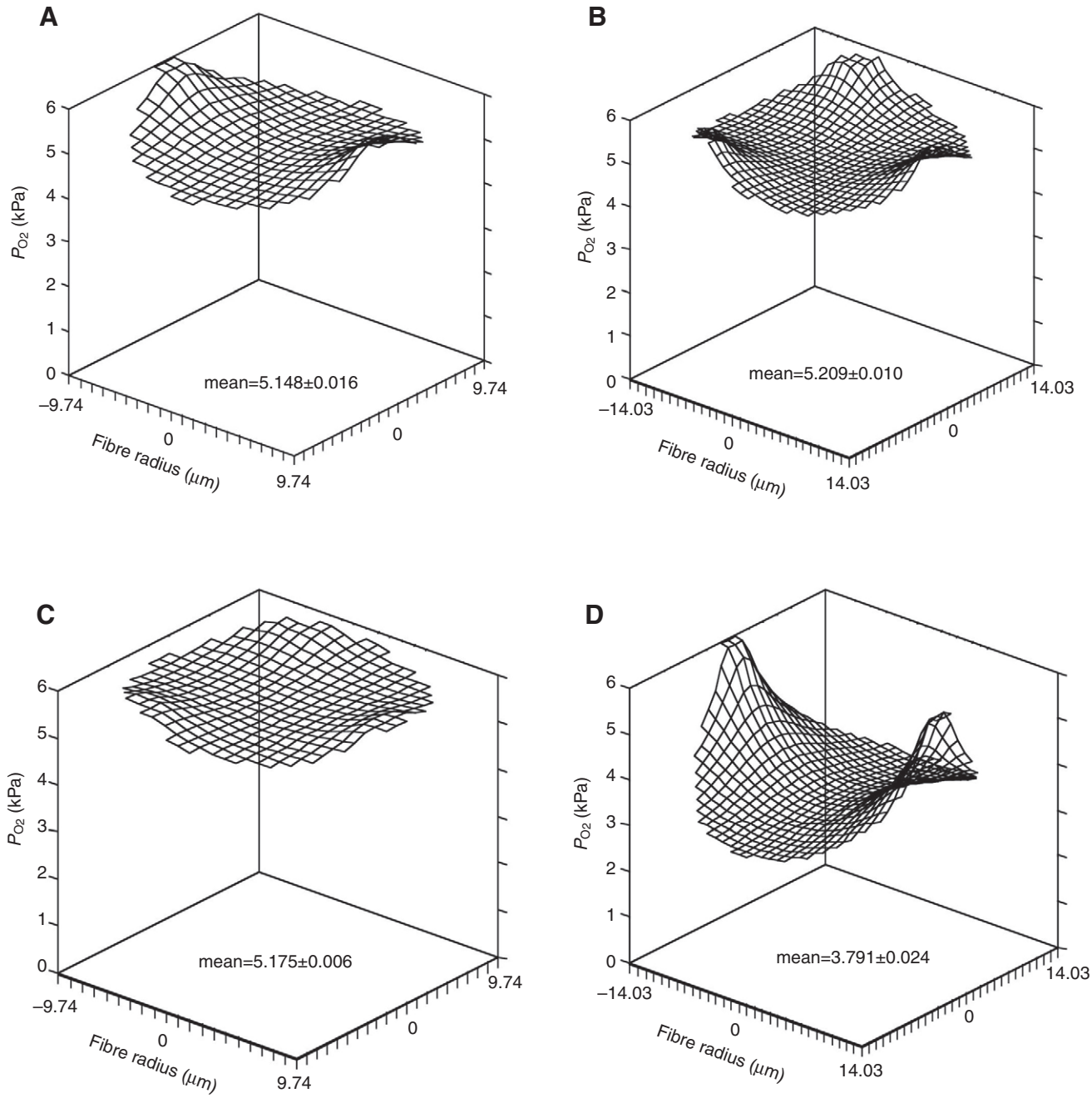

Fig. 6. Wireframe P_{O_2} plots illustrating the distribution of oxygen tension across a representative muscle fibre in (A) small and (B) large fish. The effect on oxygen tension is also shown if fibre size is reversed in (C) large and (D) small fish, without adjusting composition.

1982), but the higher V_v(mit,f) in the smallest fish on a radial distribution from a capillary suggests that oxygen delivery to support oxidative phosphorylation may decline with size in striped bass, possibly accentuated by an increase in average diffusion distances between mitochondria within growing fibres. Under steady-state, aerobic conditions it is generally agreed that the majority of cellular $\dot{M}_{O_2}$ is due to mitochondrial respiration. Oxidative enzymes show a similar negative allometric relationship (COX 52% and CS 66% reduction) to that of V_v(mit,f) (33% reduction) over the range of BM studied. Small differences between scaling of metabolic and structural indices of oxidative phosphorylation may be due to differences in allosteric modification in the former or remodelling within the latter, e.g. modifications in cristae surface area (Egginton et al., 2000; St-Pierre et al., 1998). A greater variance in mitochondrial content within the small fish indicates this size range occurs in a period of the life history of more active fibre hypertrophy, rapidly reducing V_v(mit,f) towards that found in larger fish. However, there was a twofold increase in the total mitochondrial content of individual fibres, V(mit,f), between small and large fish. Whether one views the lack of a significant allometric regression as complete compensation for changes in cell size, or the negative scaling exponent for V_v(mit,f) as a partial compensation, mitochondrial biogenesis during ontogenetic growth clearly supports the specific aerobic capacity of fibres.

The similarity of scaling patterns between V_v(mit$_{imf}$,f) and V_v(mit$_{ss}$,f) indicate they are co-regulated despite their putatively different functions, providing ATP for contractile function or active ion transport, respectively. The greater proportion of subsarcolemmal than intermyofibrillar mitochondria for a given fish size is unlikely to also provide ATP for contractile function, as diffusion rates of the ATP analogue AMP-PNP were found to be lower than those for the hexose 2-deoxyglucose (0.81 *vs* 2.14 cm^2 s^{-1}, respectively, at 15°C) (Sidell and Hazel, 1987). Changes in the exchange surface available for transport of ATP, i.e. S_v(mit,f), were less than those in V_v(mit,f), indicating that with fibre hypertrophy the population consists of proportionally fewer, larger mitochondria. Thus, if the outer membrane area limits mitochondrial respiration, e.g. at maximal O_2 consumption ($\dot{M}_{O2max}$), the aerobic capacity may be further compromised (Weibel et al., 1996) in large fish. However, a large separation of mitochondria may be accommodated if the metabolic rate is low (Kinsey et al., 2007), emphasising the need for a more holistic view of the scaling phenomenon.

Other structural remodelling

An increase in volume density of intracellular lipid in red muscle of larger eels was considered an adaptation to a more migratory lifestyle, rather than an effect of allometry (Egginton, 1986a), a conclusion supported by the lack of scaling in striped bass. Indeed, glucose-6-phosphate dehydrogenase activity showed negative scaling in *Clarias batrachus* (Tripathi and Verma, 2004), suggesting a reduction in NADPH production and hence hepatic lipogenesis, such that fuel preference may shift away from lipolysis in larger fish. However, this outcome may be dependent on diet, e.g. availability of carbohydrates, or response of other enzyme systems such as MDH.

In general, power requirements for swimming show positive allometry for both burst and sustained swimming (Goolish, 1989). Although maximising the capacity for rapid movement in small fish may be critical to their survival, as the power required for swimming varies with speed^3 the absence of positive metabolic scaling in the largest fish may suggest they are unable to generate sufficient power (Norton et al., 2000). However, the allometric increase in mean fibre area was accompanied by only a small increase in relative myofibrillar content, V_v(myo,f), although total myofibrillar content, V(myo,f), increased significantly. This suggests a greater force development per fibre with age, as power generation is proportional to total myofibril cross-sectional area. Adjustments to fibre composition mean that although the intermyofibrillar zone expands as the fish grows, this is due to an increase in myofibrils rather than other organelles, and the tight packing of muscle cells in larger fish may further enhance specific power output. From a theoretical perspective, energy consumption per unit volume is expected to show negative allometry in all vertebrates, such that cell volume and cell metabolic rate cannot both remain constant (Savage et al., 2007). Striped bass would appear to adopt the latter option for red muscle, i.e. maintain a constant cell metabolic rate but increase cell size with increasing body mass during ontogeny, consistent with scaling exponents for mass-specific metabolic rate >0 for some fish species (Clarke and Johnston, 1999). The right shift in fibre size distribution is also consistent with a dominance of hypertrophy, although the heterogeneity in both sizes indicates fibre hyperplasia occurs throughout the size range examined, possibly aiding recovery by facilitating diffusive exchange of metabolites.

Microcirculation

Although V_v(mit,f) in mammals scales with $\dot{M}_{O2max}$ (Hoppeler et al., 1980), and varies with oxidative enzyme activity in fishes (Egginton, 1998; Guderley, 2004; Sänger, 1993), these potential fluxes cannot be fully exploited unless matched by microvascular delivery of O_2. Hence, capillaries may satisfy demand for O_2 up to $\dot{M}_{O2max}$, but beyond this, glycogen stores need to be utilised to support glycolytic activity (Weibel et al., 1996). Although CD generally increases in parallel with V_v(mit,f) in vertebrates, there is considerable variability that can be attributed to the limitations of this measure of vascular supply as it is sensitive to fibre hypertrophy accompanying skeletal muscle growth (Hudlická et al., 1992). In fish, changes in skeletal muscle capillary supply are seen during development, and in response to exercise or thermal acclimation (Egginton, 1992). However, fish recruit fibre hyperplasia as well as hypertrophy during remodelling, with changes in fibre size distribution also leading to changes in C:F and oxygen supply to individual fibres that may be obscured when using global indices of capillarity, such as CD (Egginton, 1992). In trout, modest changes in various structural parameters encompassing fibre remodelling, including mitochondrial proliferation and angiogenesis, ameliorate the potentially deleterious effects of low temperature in response to seasonal acclimatisation (Egginton et al., 2000). In the American eel, an increase in C:F indicated that angiogenesis in the developing fish served to maintain aerobic capacity, while CD remained unchanged with the transition from yellow (non-migratory) to silver (migratory) morphs due to the effects of fibre hypertrophy (Egginton, 1986a). In tilapia and eel, mean fibre area varies directly with BM, whereas in red muscle CD decreased (Egginton, 1992). Ontogenetic growth thus appears to require, at best, maintenance of peripheral O_2 supply.

In striped bass, muscle fibre hypertrophy is accompanied by a compensatory angiogenesis (increasing C:F), although the compensation is incomplete (decreasing CD). Analysis of capillary structure suggests that the period of extensive developmental angiogenesis begins to wane at a body mass of around 20 g, with angiogenic indices such as endothelial sprouts (Egginton et al., 2001) showing little difference between large and small fish. Consequently, capillaries in juveniles and adults are structurally quite similar, although there was considerable variability in the data as random sampling means that capillaries can be viewed anywhere along their length, from the venular to the arteriolar side. Unlike the situation in eels (Egginton, 1992) the small increase in capillary cross-sectional area in larger striped bass was not statistically significant, similar to the situation in tilapia (Kisia and Hughes, 1992). Such changes may have important biological effects on blood flow, as resistance is proportional to the fourth power of the vessel radius, and a lower perfusion resistance due to larger lumen may offer partial compensation for vessel rarefaction in large fish. However, our calculations failed to show a significant difference in flow resistance between size classes, highlighting the need for an accurate quantification of the three-dimensional structure of the capillary bed and MABP in small fish to fully describe oxygen supply to tissue, and its adaptability.

Integrative response

The less aerobic nature of red muscle fibres in larger fish is consistent with positive scaling of glycolytic enzymes and negative scaling of oxidative enzymes. However, an increase in total mass of red muscle with size has been shown in rainbow trout (b=3.62) (Goolish, 1989) and tilapia (b=1.157) (Kisia and Hughes, 1992). Although not quantified, this was also evident in striped bass on dissection. This, in conjunction with compensatory angiogenesis, suggests that at the tissue and organism level aerobic capacity may be relatively constant, consistent with a similar calculated mean and minimum

P_{O_2} for fibres of both small and large fish. The necessity of changing fibre composition with increasing size to maintain constant oxygenation is illustrated by the lower mean and minimum P_{O_2} predicted if the fibre composition of small fish are applied to a fibre of equal size to that of large fish. If the opposite situation is modelled then the difference is small, indicating that the suite of changes accompanying fibre growth are regulated by feedback control to minimise any drop in intracellular oxygenation of larger fibres. *In vivo*, this is consistent with a hypoxia-driven stimulus for compensatory changes such as angiogenesis (Nikinmaa and Rees, 2004). Modelling a reduced capillary supply in large fish to that found in small fish decreased mean and minimum P_{O_2}, indicating that angiogenesis is a key factor in the maintenance of intramuscular oxygenation.

Conclusion

Although physical laws may dictate that structural capacities decline with increasing BM, there are many reasons why biochemical capacities vary among organisms. $\dot{M}_{O_2max}$ is an integrated outcome of disparate processes showing complementary responses, e.g. facilitated (myoglobin) and convective (capillary) delivery of O_2 show opposite allometric trends, whereas functional (enzyme) and structural (mitochondria) indices of O_2 consumption show parallel trends, suggesting a decrease of specific aerobic capacity with size. Nevertheless, as with changes in fibre size seen on temperature acclimatisation (Egginton et al., 2000), ontogenetic growth requires only modest changes to different elements in O_2 supply and demand to maintain adequate aerobic capacity of locomotory muscle in an active fish species.

LIST OF ABBREVIATIONS

$\bar{A}_f$	mean fibre area (μm^2)
b	scaling exponent
BM	body mass
CD	capillary density
C:F	capillary to fibre ratio
COX	cytochrome oxidase
CPK	creatine phosphokinase
CS	citrate synthase
ICD	intercapillary distance
LDH	lactate dehydrogenase
MABP	mean arterial blood pressure
PFK	phosphofructokinase
PK	pyruvate kinase
Re	Reynolds number
S_v	surface density
V_v	volume density (volume of object per unit volume of reference)
V_v(mit,f)	mitochondrial volume density of fibres
V_v(myo,f)	myofibrillar volume density of fibres

This work was supported by the NERC and NSF. The authors are very grateful to Bruce Sidell (University of Maine, ME, USA) for generous provision of fish and facilities for biochemical analyses, and Jennifer Molloy (University of Birmingham, UK) for assistance in analysing fibre size distribution.

REFERENCES

Bochdansky, A. B. and Leggett, W. C. (2001). Winberg revisited: convergence of routine metabolism in larval and juvenile fish. *Can. J. Fish. Aquat. Sci.* **58**, 220-230.
Burness, G. P., Leary, S. C., Hochachka, P. W. and Moyes, C. D. (1999). Allometric scaling of RNA, DNA, and enzyme levels: an intraspecific study. *Am. J. Physiol.* **277**, R1164-R1170.
Childress, J. J. and Somero, G. N. (1990). Metabolic scaling – a new perspective based on scaling of glycolytic enzyme activities. *Am. Zool.* **30**, 161-173.
Clarke, A. and Johnston, N. M. (1999). Scaling of metabolic rate with body mass and temperature in teleost fish. *J. Anim. Ecol.* **68**, 893-905.
Davies, R. and Moyes, C. D. (2007). Allometric scaling in centrarchid fish: origins of intra- and inter-specific variation in oxidative and glycolytic enzyme levels in muscle. *J. Exp. Biol.* **210**, 3798-3804.
Degens, H., Deveci, D., Botto-van Bemden, A., Hoofd, L. J. and Egginton, S. (2006). Maintenance of heterogeneity of capillary spacing is essential for adequate oxygenation in the soleus muscle of the growing rat. *Microcirculation* **13**, 467-476.
Egginton, S. (1986a). Metamorphosis of the American eel, *Anguilla rostrata* Le Seur: II. Structural reorganisation of the locomotory musculature. *J. Exp. Zool.* **238**, 297-309.
Egginton, S. (1986b). Metamorphosis of the American eel, Anguilla rostrata LeSeur: I. Changes in metabolism of skeletal muscle. *J. Exp. Zool.* **237**, 173-184.
Egginton, S. (1990). Morphometric analysis of tissue capillary supply. In *Advances in Comparative and Environmental Physiology*, vol. 6 (ed. R. G. Boutilier), pp. 75-141. Berlin Heidelberg: Springer-Verlag.
Egginton, S. (1992). Adaptability of the anatomical capillary supply to skeletal muscle of fishes. *J. Zool.* **226**, 691-698.
Egginton, S. (1998). Anatomical adaptations for peripheral oxygen transport at high and low temperatures. *S. A. J. Zool.* **33**, 119-128.
Egginton, S. (2002). Temperature and angiogenesis: the possible role of mechanical factors in capillary growth. *Comp. Biochem. Physiol.* **132A**, 773-787.
Egginton, S. and Cordiner, S. (1997). Cold-induced angiogenesis in seasonally acclimatized rainbow trout (*Oncorhynchus mykiss*). *J. Exp. Biol.* **200**, 2263-2268.
Egginton, S. and Johnston, I. A. (1982). A morphometric analysis of regional differences in myotomal muscle ultrastructure in the juvenile eel (*Anguilla anguilla* L.). *Cell Tissue Res.* **222**, 579-596.
Egginton, S. and Rankin, J. C. (1998). Vascular adaptations for a low pressure/high flow blood supply to locomotory muscles of Antarctic icefish. In *Fishes of Antarctica. A biological overview (*ed. G. di Prisco E. Pisano and A. Clark), pp. 185-195. Italy: Springer-Verlag.
Egginton, S. and Sidell, B. D. (1989). Thermal acclimation induces adaptive changes in subcellular structure of fish skeletal muscle. *Am. J. Physiol. Regul. Integr. Comp. Physiol.* **256**, R1-R9.
Egginton, S., Cordiner, S. and Skilbeck, C. (2000). Thermal compensation of peripheral oxygen transport in skeletal muscle of seasonally acclimatized trout. *Am. J. Physiol. Regul. Integr. Comp. Physiol.* **279**, R375-R388.
Egginton, S., Zhou, A. L., Brown, M. D. and Hudlická, O. (2001). Unorthodox angiogenesis in skeletal muscle. *Cardiovasc. Res.* **49**, 634-646.
Ewart, H. S. and Driedzic, W. R. (1987). Enzymes of energy metabolism in salmonid hearts: spongy versus cortical myocardia. *Can. J. Zool.* **65**, 623-627.
Ewart, H. S., Canty, A. A. and Driedzic, W. R. (1988). Scaling of cardiac oxygen consumption and enzyme activity levels in sea raven (*Hemitripterus americanus*). *Physiol, Zool,* **61**, 50-56.
Garenc, C., Coutrure, P., Laflamme, M.-A. and Guderley, H. (1999). Metabolic correlates of burst swimming capacity of juvenile and adult three-spine stickleback (*Gasterosteus aculeatus*). *J. Comp. Physiol. B* **169**, 113-122.
Glazier, D. S. (2005). Beyond the '3/4-power law': variation in the intra- and interspecific scaling of metabolic rate in animals. *Biol. Rev.* **80**, 611-662.
Goolish, E. M. (1989). The scaling of aerobic and anaerobic muscle power in rainbow trout (*Salmo gairdneri*). *J. Exp. Biol.* **147**, 493-505.
Goolish, E. M. (1991). Anaerobic swimming metabolism of fish: sit-and-wait versus active forager. *Physiol. Zool.* **64**, 485-501.
Guderley, H. (2004). Locomotor performance and muscle metabolic capacities: impact of temperature and energetic status. *Comp. Biochem. Physiol.* **139B**, 371-382.
Hoofd, L. and Egginton, S. (1997). The possible role of intracellular lipid in determining oxygen delivery to fish skeletal muscle. *Respir. Physiol.* **107**, 191-202.
Hoppeler, H., Mathieu, O. and Lindstedt, S. L. (1980). Scaling structural parameters of oxygen consumption in muscle against VO_{2max} and body mass. In *Exercise Bioenergetics and Gas Exchange* (ed. P. Cerretelli and B. J. Whipp), pp. 129-135. Symposium of the Giovanni Lorenzini Foundation. Oxford: Elsevier.
Hoppeler, H., Mathieu, O., Weibel, E. R., Kramer, R., Lindstedt, S. L. and Taylor, C. R. (1981). Design of the mammalian respiratory system VIII. Capillaries in skeletal muscles. *Respir. Physiol.* **44**, 129-150.
Hudlická, O., Brown, M. and Egginton, S. (1992). Angiogenesis in skeletal and cardiac muscle. *Physiol. Rev.* **72**, 369-417.
Kerr, J. E. (1953). *Studies of fish preservation at the Contra Costa steam plant of the Pacific Gas and Electric Company*. 66pp. California Department of Fisheries and Game Bulletin 92. Sacramento, California.
Kinsey, S. T., Hardy, K. M. and Locke, B. R. (2007). The long and winding road: influences of intracellular metabolite diffusion on cellular organization and metabolism in skeletal muscle. *J. Exp. Biol.* **210**, 3505-3512.
Kisia, S. M. and Hughes, G. M. (1992). Red muscle fibre and capillary dimensions in different sizes of a tilapia, *Oreochromis niltoicus* (Trewavas). *J. Fish Biol.* **40**, 97-106.
Martinez, M., Dutil, J.-D. and Guderley, H. (2000). Longitudinal and allometric variation in indicators of muscle metabolic capacities in Atlantic cod (*Gadus morhua*). *J. Exp. Zool.* **287**, 38-45.
McHenry, M. J. and Lauder, G. V. (2005). The mechanical scaling of coasting in zebrafish (*Danio rerio*). *J. Exp. Biol.* **208**, 2289-2301.
Mitchell, S. J. and Cech, J. J. (1994). Comparison of metabolic rates of striped bass, white bass, and their hybrid at selected temperatures and dissolved oxygen levels. *http://www-heb. pac. dfo-mpo. gc. ca/congress/1994/mitchell. pdf* (access 03/09).
Nikinmaa, M. and Rees, B. B. (2004). Oxygen-dependent gene expression in fishes. *Am. J. Physiol.* **288**, 1079-1090.
Norton, S. F., Eppley, Z. A. and Sidell, B. D. (2000). Allometric scaling of maximal enzyme activities in the axial musculature of striped bass, *Morone saxatilis* (Walbaum). *Physiol. Biochem. Zool.* **73**, 819-828.
Pörtner, H. O. (2002). Physiological basis of temperature-dependent biogeography: trade-offs in muscle design and performance in polar ectotherms. *J. Exp. Biol.* **205**, 2217-2230.
Poupa, O., Lindstrom, L., Maresca, A. and Tota, B. (1981). Cardiac growth, myoglobin, proteins and DNA in developing tuna (*Thunnus thynnus thynnus* L.). *Comp. Biochem. Physiol.* **70A**, 217-222.
Rodnick, K. J. and Sidell, B. D. (1995). Effects of body size and thermal acclimation on parvalbumin concentration in white muscle of striped bass. *J. Exp. Zool.* **272**, 266-274.

Sandblom, E. and Axelsson, M. (2005). Baroreflex mediated control of heart rate and vascular capacitance in trout. *J. Exp. Biol.* **208**, 821-829.
Sänger, A. M. (1992). Quantitiative fine structural diversification of red and white muscle fibres in cyprinids. *Environ. Biol. Fishes* **33**, 97-104.
Sänger, A. M. (1993). Limits to the acclimation of fish muscle. *Rev. Fish Biol. Fisheries* **3**, 1-15.
Savage, V. M., Allen, A. P., Brown, J. H., Gillooly, J. F., Herman, A. B., Woodruff, W. H. and West, G. B. (2007). Scaling of number, size, and metabolic rate of cells with body size in mammals. *Proc. Natl. Acad. Sci. USA* **104**, 4718-4723.
Schmidt-Nielsen, K. (1984). *Scaling. Why is animal size so important?* Cambridge: Cambridge University Press.
Sidell, B. D. and Hazel, J. R. (1987). Temperature affects the diffusion of small molecules through cytosol of fish muscle. *J. Exp. Biol.* **129**, 191-203.
Sidell, B. D. and Moerland, T. S. (1989). Effects of temperature on muscular function and locomotory performance in teleost fish. In *Adv. Comp. Environ. Physiol.*, vol. 5, pp. 115-155. Berlin: Springer-Verlag.
Somero, G. N. and Childress, J. J. (1980). A violation of the metabolism-size scaling paradigm: activities of glycolytic enzymes in muscle increase in larger-size fish. *Physiol. Zool.* **53**, 322-337.
St-Pierre, J., Charest, P.-T. and Guderley, H. (1998). Relative contribution of quantitative and qualitative changes in mitochondria to metabolic compensation during seasonal acclimation of rainbow trout *Oncorhynchus mykiss*. *J. Exp. Biol.* **201**, 2961-2970.
Suarez, R. K. and Darveau, C. A. (2005). Multi-level regulation and metabolic scaling. *J. Exp. Biol.* **208**, 1627-1634.
Sullivan, K. M. and Somero, G. N. (1983). Size- and diet-related variations in enzymic activity and tissue composition in the sablefish, *Anoplopoma fimbria*. *Biol. Bull.* **164**, 315-326.
Torres, J. J. and Somero, G. N. (1988). Metabolism, enzymic activities and cold adaptation in Antarctic mesopelagic fishes. *Mar. Biol.* **98**, 169-180.
Tripathi, G. and Verma, P. (2004). Scaling effects on metabolism of a teleost. *J. Exp. Zool.* **301A**, 718-726.
Walsh, P. J., Bedolla, C. and Mommsen, T. P. (1989). Scaling and sex-related differences in toadfish (*Opsanus beta*) sonic muscle enzyme activities. *Bull. Mar. Sci.* **45**, 68-75.
Weibel, E. R. (1979). *Stereological methods: Practical methods for biological morphometry*. London: Academic Press.
Weibel, E. R., Taylor, C. R., Weber, J.-M., Vock, R., Roberts, T. J. and Hoppeler, H. (1996). Design of the oxygen and substrate pathways VII. Different structural limits for oxygen and substrate supply to muscle mitochondria. *J. Exp. Biol.* **199**, 1699-1709.
West, G. B., Brown, J. H. and Enquist, B. J. (1997). A general model for the origin of allometric scaling laws in biology. *Science* **276**, 122-126.
West, G. B., Brown, J. H. and Enquist, B. J. (1999). The fourth dimension of life: fractal geometry and allometric scaling of organisms. *Science* **284**, 1677-1679.
West, G. B., Woodruff, W. H. and Brown, J. H. (2002). Allometric scaling of metabolic rate from molecules and mitochondria to cells and mammals. *Proc. Natl. Acad. Sci. USA* **99 Suppl. 1**, 2473-2478.
White, C. R. and Seymour, R. S. (2005). Sample size and mass range effects on the allometric exponent of basal metabolic rate. *Comp. Bioch. Physiol.* **142A**, 74-78.
White, C. R., Phillips, N. F. and Seymour, R. S. (2006). The scaling and temperature dependence of vertebrate metabolism. *Biol. Lett* **2**, 125-127.
White, C. R., Cassey, P. and Blackburn, T. M. (2007). Allometric exponents do not support a universal metabolic allometry. *Ecology* **88**, 315-323.
Wuenschel, M. J., Werner, R. G. and Hoss, D. E. (2004). Effect of body size, temperature, and salinity on the routine metabolism of larval and juvenile spotted seatrout. *J. Fish Biol.* **64**, 1088-1102.